EUROPEAN LABORATORY FOR PARTICLE PHYSICS

CERN / SPSC 99–15
SPSC / I 221
7 May 1999

Letter of Intent

Study of Dimuon and Charm Production with Proton and Heavy Ion Beams at the CERN SPS

C. Cicalo, A. De Falco, M.P. Macciotta, A. Masoni, G. Puddu, S. Serci and G. Usai
Università di Cagliari and INFN, Cagliari, Italy.

V. Granata[1)], E. Heijne, C. Lourenço[*)], V.G. Palmieri, I. Ropotar[2)] and
P. Sonderegger[*,3)]
CERN, Geneva, Switzerland.

A. Baldit, J. Castor, A. Devaux, B. Espagnon, J. Fargeix, P. Force and P. Saturnini
LPC, Univ. Blaise Pascal and CNRS-IN2P3, Clermont-Ferrand, France.

M.C. Abreu[4)], P. Bordalo[3)], L. Casagrande, C. Quintans, S. Ramos[3)],
P. Rato-Mendes[4)], R. Shahoyan[5)] and S. Silva
LIP, Lisbon, Portugal.

M.P. Comets, D. Jouan, Y. Le Bornec, M. Mac Cormick and N. Willis
IPN, Univ. de Paris-Sud and CNRS-IN2P3, Orsay, France.

B. Chaurand and L. Kluberg
LPNHE, Ecole Polytechnique and CNRS-IN2P3, Palaiseau, France.

R. Arnaldi, P. Cortese, N. De Marco, A. Musso and E. Scomparin
Università di Torino and INFN, Turin, Italy.

V. Danielyan, A.A. Grigorian, S. Grigoryan, H. Gulkanyan and H. Vardanyan
YerPhI, Yerevan, Armenia.

[*)] Contactpersons

[1)] Also at Brunel University, Brunel, England
[2)] Also at Wupertal University, Wupertal, Germany
[3)] Also at IST, Universidade Técnica de Lisboa, Lisbon, Portugal
[4)] Also at UCEH, Universidade do Algarve, Faro, Portugal
[5)] On leave from YerPhI, Yerevan, Armenia

Contents

1 Introduction

We propose hereafter an experiment to perform a systematic and accurate study of dimuon production in heavy ion collisions, by adding a magnetic vertex spectrometer to the NA50 experiment. Besides studying low mass dimuon production with good mass resolution, we intend to measure the production rate of charmed mesons, through their semileptonic decay, by measuring the offset of the muon tracks extrapolated to the interaction point.

In a few weeks of running, the experiment will be able to collect enough statistics to study the behaviour of low mass dimuons (and, in particular, of the ρ, ω and ϕ resonances) as a function of the centrality of the collision, measured event by event through the charged particle multiplicity and, independently, through the forward energy detected in a Zero Degree Calorimeter, ZDC. The expected statistics and acceptance as a function of the dimuon transverse momentum will also enable us to make a detailed study of the low mass resonance production as a function of p_{T}, for peripheral and central Pb-Pb collisions.

With a mass resolution of around 20 MeV at the ω mass, we will be able to separately study the production of ω and ρ mesons, and search for a mass shift and broadening of the short-lived ρ meson, from p-Be to Pb-Pb and from peripheral to central Pb-Pb collisions, as a function of transverse momentum.

Such measurements can be considered as a natural continuation of the dilepton physics program of the NA38/NA50, Helios-3 and CERES experiments. In particular, the CERES experiment has measured low mass di-electron production from p-Be to Pb-Au, at the SPS, finding intriguing evidence for a rather large enhancement of e^+e^- pairs in the mass region 0.2–0.7 GeV, motivating a very active theoretical research in recent years.

The second physics topic we intend to explore concerns the production of intermediate mass dimuons. The NA38/NA50 and Helios-3 experiments have observed an enhanced production of dimuons with mass between 1.2 and 2.5 GeV. The experiment proposed in this document will be able to clarify if this excess production is due to prompt dimuons or to muon pairs which originate at some distance from the event vertex. The tool is a measurement of the 'offset' of the muon tracks relative to the interaction point (in charm experiments this quantity is often named 'impact parameter'). This measurement will be able to rule out one of the two hypothetical explanations currently considered: an enhancement of charm production or the production of thermal dimuons. The physics motivation of the proposed experiment will be described in more detail in section 2.

The proposed experiment should be considered as an upgrade of the existing NA50 experiment. We will use the NA50 dimuon spectrometer, ZDC and beam line as they exist today. The target region, however, will be rebuilt. The cornerstone of the new vertex spectrometer is the forthcoming Alice1 pixel chip. While having been developed for ALICE, it has turned out to be ideally suited for the special needs of the experiment proposed here. An existing dipole magnet will house a number of pixel

planes totalling $\sim 10^6$ silicon pixel channels and covering the angular acceptance of the NA50 muon spectrometer. In addition, we will use a new beam tagging detector, made of silicon microstrips operated near 100 K. The experimental apparatus will be described in section 3, with particular attention to the new detectors.

By measuring the muon tracks before they enter the hadron absorber, the new silicon pixel telescope will greatly improve the physics performance of the dimuon spectrometer, in terms of mass resolution and signal to background ratio. The dipole field in the vertex region will enhance the acceptance of low $m_{\rm T}$ dimuons. The pointing accuracy of the planned setup will allow to measure the transverse offset of each muon track, at the origin, with a resolution better than 50 μm, good enough to select an event sample highly enriched by simultaneous semileptonic decays of $D\overline{D}$ pairs.

The performance of this new detector concept in dimuon spectrometry has been evaluated by simulation, as will be described in section 4. Also, a prototype pixel spectrometer has been built, using the existing LHC1 chip, and exposed in 1998 to proton and lead beams. First results of these feasibility tests will be presented in section 5.

If supported by the SPSC, the experiment would be ready to take first data at the end of the lead ion beam period of year 2000, as soon as the NA50 experiment finishes the data taking needed to complete its J/ψ physics programme.

2 Physics Programme

It is important to situate the goals of this experiment in the context of the present heavy ion physics programme at CERN. It is widely accepted in the community that the heavy ion programme at the SPS has recently reached a very exciting stage. Thanks to the important developments provided by the Pb beam, the present collection of experimental results provides strong support for the expectation that matter with a structure radically different from nuclear or hadronic matter is created in Pb-Pb collisions at the SPS.

The present status was reviewed in a dedicated workshop, attended by representatives of all the CERN experiments, held in Chamonix in September 1998. The community expressed [1] growing confidence that the present indications of quark matter formation in ion collisions at the SPS may be fully clarified with the data already collected in 1998 or to be added in the running periods of 1999 and 2000. The most striking experimental observations concern the suppression of J/ψ production, the excess emission of lepton pairs in the mass range below the ρ resonance and the enhanced production of multi-strange hadrons.

2.1 J/ψ suppression

The earlier evidence provided by NA50 for an anomalous mechanism of J/ψ suppression in Pb-Pb collisions [2] was confirmed by a new data analysis [3], comparing the

centrality dependence of the J/ψ cross section to the minimum bias spectra (rather than to the Drell-Yan process). The results clearly reveal that the J/ψ production in central Pb-Pb collisions is strongly suppressed with respect to the pattern observed in the peripheral collisions and in the data of lighter systems. The observation of a threshold behaviour (in a single collision system) is a clear indication for the transition to deconfined QCD matter [4]. In fact, two consecutive thresholds are expected to occur, due to the dissolution of the χ_c and J/ψ states at different energy densities.

However, the final interpretation of these observations would considerably benefit from direct and independent knowledge about the gluon content of the matter produced in the early stages of the heavy ion collisions. Such information would be provided by a measurement of charmed meson production, as performed by the experiment we are proposing. Indeed, due to the large mass of the c quark, charmed mesons are predominantly produced (by gluon fusion) in the early hard scattering processes. Besides helping to clarify the mechanisms of production and suppression of the bound $c\bar{c}$ charmonia states, a good knowledge on the gluon content is also essential to the understanding of the quark-*gluon* plasma properties.

2.2 Low-mass lepton pairs

The CERES experiment has confirmed that the measured yield of low mass e^+e^- pairs, in Pb-Au collisions, exceeds by a factor of 3 or 4 the expected signal from hadronic decays [5]. The excess dileptons are concentrated at low p_{T} and their yield scales with the square of the charged particle multiplicity. Dileptons from $\pi^+\pi^-$ annihilations cannot account for the observed shape of the excess yield.

These observations are consistent with the expectation that the properties of the vector mesons should change when produced in dense matter, due to medium effects. In particular, near the phase transition to the quark-gluon phase, partial restoration of chiral symmetry should induce changes in the masses and decay widths of the mesons. The short lifetime of the ρ meson, shorter than the expected lifetime of the dense system produced in the SPS heavy ion collisions, makes it a sensitive probe of medium effects and, in particular, of chiral symmetry restoration.

Clearly, high precision data are needed to distinguish between the different theoretical models and to determine the relation between the present observations and chiral symmetry restoration. Such data should be able to separate the ω from the ρ, with a good signal to background ratio, and should have enough statistics to allow a detailed study of the observed behavior as a function of centrality and transverse momentum.

Thanks to the very clean and highly selective dimuon trigger, the experiment we are proposing should collect (in the final analysis data sample) more than 200 000 ρ, ω, and ϕ events per week, with a mass resolution around 20 MeV and a signal to background ratio around 1:1 in the resonance peaks.

2.3 Strangeness enhancement

The observation of enhanced production of strangeness in nuclear collisions is now well established, in particular thanks to the precise measurement of the Λ, Ξ and Ω yields in Pb-Pb collisions, by the WA97 experiment [6]. The enhancement of the hyperon yields, relative to the p-Be and p-Pb values, grows with the strangeness content, culminating in an enhancement factor of more than a factor 15 for the $\Omega+\overline{\Omega}$. The observations follow the behavior expected if the strange quarks were equilibrated in a deconfined and chirally symmetric quark-gluon plasma.

Depending on the energy density reached in the early stages of the SPS heavy ion collisions, charm production could be similarly enhanced relative to the normal extrapolation of the nucleon-nucleon yields.

2.4 Charm production

The production of charm quarks leads mainly to correlated pairs of D and $\overline{D}$ mesons. Only a few percent of the charmed quark pairs end up in the bound charmonia states presently studied by the NA50 experiment.

The NA38/NA50 and Helios-3 experiments have observed that the dimuon continuum between the ϕ and the J/ψ is enhanced in heavy ion collisions, with respect to the expected superposition of Drell-Yan and $D\overline{D}$ sources, which neatly explain the p-A data. It has been shown [7] that an enhancement of the charm production cross-section would explain the observations, providing a reasonable description of the mass and p_{T} distributions of the measured data. While these observations are still the subject of much debate, it is clear that an enhancement of charm production in heavy ion collisions would have direct implications on the interpretation of the charmonia data, boosting the anomaly of the measured J/ψ suppression.

The present situation reinforces the importance of having a direct measurement of open charm production in heavy ion collisions. Such a measurement requires a dedicated SPS experiment, that can cope with the high particle multiplicities reached in the most central Pb-Pb collisions (almost 400 charged particles per unit rapidity at midrapidity) and with the small D production cross section. The highly selective dimuon trigger of the experiment proposed here will enable us to take full advantage of the high intensity beam line in ECN3 (providing up to 10^7 Pb-Pb collisions per burst) to study this rare process.

The potential of our experiment for measuring the D meson production yield (and its centrality dependence) is being studied by Monte Carlo simulation. The results, presented in section 4, show that an open charm measurement with proton and lead beams is feasible at the SPS. If done in the running periods of years 2001 and 2002, this experiment would keep the CERN heavy ion physics programme competitive with respect to the RHIC experiments.

2.5 p-A physics

This experiment will also be able to provide new insight into several issues of dimuon production in p-A collisions. In particular, it will be able to separately study the two main sources of muon pairs contributing to the continuum in the mass window between the ϕ and the J/ψ resonances. A clean measurement of prompt dimuon production at such low masses, covering a broad range in $p_{\rm T}$, will help to clarify the $q\bar{q}$ annihilation (Drell-Yan) process down to a Q^2 scale close to 1 GeV^2.

In more general terms, we will be able to investigate if the low mass prompt dimuon continuum can be calculated in next-to-leading-order QCD, and evaluate the importance of the so-called higher twist effects. This study can also be done in a sub-sample of high transverse momentum dileptons, for which the QCD calculation is both simpler and more reliable. Furthermore, it has recently been proposed [8] that the study of dileptons with $p_{\rm T}$ greater than roughly half their mass, mainly produced by subprocesses initiated by gluons, is a good source of information on the gluon momentum density, complementing the complicated studies of inclusive real photon production.

In this context we should recall that the low mass dimuon spectrum measured by the NA38 experiment, in p-U collisions, exceeds the sum of the expected sources (the "hadronic cocktail" plus the $D\overline{D}$ decays) by $\sim$40 % in the mass range 400–650 MeV [9]. The observed "excess" increases with the dimuon $p_{\rm T}$, indicating the presence of a harder source of dileptons in this mass window, possibly related to $q\bar{q}$ annihilation.

Another interesting "proton physics" prospect of the proposed experiment is the measurement of the branching ratio of the ω decay in $\mu^+\mu^-$, not yet measured up to now, and the related study of ρ-ω interference.

We intend to investigate in the near future if the new detector can also study χ_c production, through the radiative decay $\chi_c \rightarrow \psi + \gamma$, measuring the e^+e^- converted photons with the silicon pixel spectrometer. A measurement of the A-dependence of χ_c production, in p-A collisions, would be a rather interesting measurement to do, in particular in the context of the χ_c production in heavy ion collisions, with clear implications on the understanding of the J/ψ suppression.

3 Experimental Apparatus

The experiment proposed in this document will mainly consist of two detector components: the muon spectrometer presently used in the NA50 experiment and a new silicon vertex telescope, to be placed in the target region inside a dipole magnet. The experiment is completed by a zero degree calorimeter, inherited from NA50, which will measure the impact parameter of the heavy ion collisions. A detailed description of the ZDC is available in Ref. [10].

The new silicon vertex telescope, although small in size (20 cm long, to be compared with the 20 m long muon spectrometer), will significantly improve the physics

capability of the experiment. Its several planes of silicon pixel detectors will cover the angular acceptance of the dimuon spectrometer. We also intend to use a cold microstrip beam detector, placed upstream of the target, which will measure the transverse coordinates of the incoming Pb ions with a precision of ~ 15 μm.

3.1 The muon spectrometer

The core of the NA50 experiment is the muon spectrometer, designed for the NA10 experiment and optimised for the measurement of high mass muon pairs. It covers the pseudo-rapidity interval $2.8 < \eta_{\rm lab} < 4.0$. The angles and momenta of the muon tracks are measured in two sets of multi-wire proportional chambers, placed before and after an air gap toroidal magnet. The dimuon trigger is provided by coincidences among four scintillator hodoscopes.

The muon spectrometer is shielded from the high multiplicity target region by a 5.4 m long hadron absorber, made mainly of graphite. Its first 60 cm are made of denser materials (BeO or Al_2O_3), to absorb the pions and kaons before they decay to muons, leading to the combinatorial background of uncorrelated (like-sign and opposite-sign) muon pairs, which cause most of the triggers. The muons must traverse a final 1.2 m iron wall before reaching the last trigger hodoscope, increasing to 4 GeV the minimum energy of the detected muons. A detailed description of the design and phase space coverage of the spectrometer can be found in Ref. [11].

The absorber configuration (some of its carbon sections can be replaced by iron) and the strength of the magnetic field play an important role in defining the dimuon acceptance, trigger rate and background rejection.

For the low mass dimuon physics program we plan to collect data with a current of 3000 A in the toroidal magnet and with 20 cm of iron at the end of the muon filter. For the charm production study the setup will be optimised by increasing the current in the toroidal magnet to 4000 A and by including 80 cm of iron in the muon filter, thereby suppressing the low mass dimuons and reducing the trigger rate by about a factor of 5.

3.2 The pixel vertex spectrometer

The main component of the new experimental setup is a vertex spectrometer, made of several planes of silicon pixels detectors, placed upstream of the dimuon spectrometer currently used in the NA50 experiment.

We will use the Alice1 pixel readout chip, developed in the framework of the ALICE experiment. This chip will be produced in commercial CMOS 0.25 μm technology, which has been shown to survive even after a radiation dose of ~ 30 Mrad [12].

Its total sensitive area of 12.8×9.6 mm^2 is segmented into 256×32 pixels of 50×300 μm^2. Being designed for LHC running, a strobe width of 50 ns is achievable for the asynchronous SPS operation. Other remarkable features are the possibility to adjust individually the threshold of each pixel and the automatic leakage current

compensation, also for each pixel. The latter is essential to cope with the extremely inhomogeneous irradiation present in a fixed target geometry. In summary, the Alice1 chip fulfils the requirements of our experiment in terms of spatial resolution, timing and radiation tolerance.

The silicon pixel telescope is placed inside an existing dipole magnet (named TC8), of overall length 55 cm and 8 cm horizontal gap. The horizontal 1.67 T field extend over a region of 25 cm along the beam axis. The first 60 cm long Al_2O_3 section of the hadron absorber starts at 26 cm from the target, still inside the magnet.

The layout of the telescope is depicted in Fig. 1. We are currently considering a layout with eight pixel planes placed at 8, 9, 10, 11, 15, 17, 22 and 24 cm from the target. Half of them are Y planes, which have the rectangular pixels oriented in such a way as to measure the y coordinate with high accuracy, $\sigma_y \sim 15$ μm, and thereby achieve optimal momentum resolution. In order to reach the wanted accuracy in the extrapolation to the vertex also in x, the planes 2 and 4 are X planes, while the last two are U and V planes, tilted relative to the vertical position, in the $x - y$ plane, by an angle of around $\pm 30°$. A total number of 86 chips is enough to complete the 8 planes of the pixel telescope, covering the angular acceptance of the dimuon spectrometer (between 40 and 120 mrad). Using the present technology, each plane introduces a thickness of 1.1 % X_0 in the path of the particles it measures.

The measurement of D meson production relies on the identification of muon tracks that do not point to the interaction point. We designate by "offset" the distance, in the transverse plane, between the extrapolated muon track and the interaction point. To select an event sample dominated by muon pairs from semileptonic D decays, we must be able to measure the track offset with a resolution of at least 50 μm (for comparison, the $c\tau$ is 317 μm for the $D^{\pm}$ and 124 μm for the $D^0/\overline{D^0}$).

Figure 2 shows how the offset resolution in both transverse coordinates depends on the distance between the first telescope plane and the target (keeping the other planes in their nominal positions). As expected, the offset resolution improves when the first plane is placed closer to the target, but even at 10 cm it would lead to a reasonable selection of $D\overline{D}$ events, using both y and x offset information.

Figure 3 shows the $1/r^2$ dependence of the occupancy (determined as the number of pixels hit over the total number of pixels in the plane) on the radial distance r from the beam axis, for three different z positions (5, 8 and 20 cm from the target). The calculation has been done using a gaussian rapidity distribution, of width $\sigma = 1.5$, and for two values of charged particle multiplicity, corresponding to average and head-on Pb-Pb collisions of 158 GeV per incident nucleon (rapidity density at midrapidity of 120 and 450 charged particles, respectively).

Figure 4 shows the occupancy for head-on Pb-Pb collisions, within the angular acceptance of the dimuon spectrometer. From these results we are confident that, placing the first plane at 8 cm from the target, the occupancy in the pixel planes is always below 10 % even for the most central collisions and in the area closer to the beam axis. This ensures that the track reconstruction in the vertex spectrometer can be performed with good efficiency over the full geometrical acceptance.

In order not to have any material in the beam axis, which would result in an undesirable target, the pixel chips of the first plane are placed at a distance of 1 mm from the beam axis. This implies that the active detector area starts at 2 mm from the beam axis, limiting the geometrical acceptance for dimuon events, in the first plane, to around 80 %.

We have computed the integrated radiation dose accumulated in the pixel planes, assuming the following running conditions: a beam intensity of 5×10^7 Pb ions per burst; a target thickness of 10 % $\lambda_{\rm int}$; and a running efficiency of 80 %. Figure 5 shows the dose affecting the first plane, the most irradiated one, as a function of the radial distance from the beam axis. In the most exposed regions, which receive about 10 times more radiation than the outer areas, the radiation dose should be around 1 Mrad per running week.

Since the Alice1 chip has already been shown to tolerate up to 30 Mrad (as described above) and since it is able to cope with a very inhomogeneous radiation dose, we do not anticipate any problems from radiation damage in the readout electronics. In order to decrease the leakage current of the detector and to prevent early degradation of the charge collection efficiency (due to reverse annealing), the pixel planes will be kept at around $-20\,^{\circ}$C.

A GEANT simulation has been performed to estimate the background from δ rays and secondary particles produced in the magnet material. The results show that most of the δ-rays are swept away by the dipole field and do not reach the detectors, while the contribution from secondaries is negligible, increasing by less than 10 % the number of hits in the last plane.

3.3 The beam-scope

In order to measure the transverse coordinates of each incoming lead ion, we will insert a "beam-scope" in the beam axis, upstream of the target. This measurement will provide a strict constraint in the determination of the interaction point, inside the target, relative to which the offset of the muon tracks will be determined.

The requirements imposed on this detector are very demanding in terms of radiation tolerance, readout speed and spatial resolution. We need to measure the line of incidence of each incoming Pb ion, at a rate of around 10^7 ions per second, and with a spatial resolution of around 20 μm in both transverse coordinates.

The beam-scope is formed by two stations placed at 20 cm and 10 cm upstream of the target. Each station is composed by an x and a y plane of single-sided 50 μm pitch silicon microstrips. The design of one such plane is shown in Fig. 6. With traditional techniques, a silicon detector would not stand the expected radiation dose. We intend to use the technology of cryogenic silicon detectors, recently developed by the RD39 collaboration. Indeed, it has been shown [13] that the radiation tolerance of silicon detectors can be greatly improved if the operating temperature is below $\sim$130 K, the tracking properties remaining unaffected even after very high fluencies [14]. We plan to cool the four planes of silicon microstrips by liquid nitrogen, and to install them

in a vaccum tube, mechanically connected to the beam pipe.

Each microstrip is connected to a fast current amplifier, which preserves the intrinsic timing of the signal (about 5 ns, as measured in the November 1998 test run described in section 5.2). The output of the amplifier will go to a fast digital pipe-line for signal processing. Therefore, the counting losses will be negligible up to 5×10^7 Pb ions per 4.8 s spill.

In the case of proton collisions, where the charged particle multiplicity is much smaller, the determination of the interaction point can be precisely done simply by fitting the tracks in the vertex spectrometer. Since the proton running does not require the operation of the beam-scope, its readout electronics has been optimised for the Pb running conditions.

3.4 Data acquisition and analysis

In order to achieve the goals of the proposed experiment, the data acquisition system presently in use in the NA50 experiment will be upgraded. Considerable work in this respect has already been performed to cope with the requirements of the feasibility tests done in 1998. Further changes will be introduced to adapt the system to the specifications of the Alice1 chip. In what concerns the (VME) readout electronics, we will profit from the work done for the Alice experiment.

The data acquisition requirements of this experiment do not require any specific new developments and we will profit from solutions implemented in currently running experiments as, for instance, NA48.

The expected event size for average Pb-Pb collisions is around 10 kbyte. Assuming a trigger rate of 1 kHz ($\sim$4000 events per spill), we anticipate a data flow of 40 Mbyte per burst. We plan to store this information in a VME memory buffer during the burst, using the SPS cycle of 19 s to write the data in permanent storage media. With this data rate, we should collect about 150 Gbyte of data per day, or $\sim$1 Terabyte per week of Pb-Pb running, which we plan to store using CERN's central data recording system.

We will request from the CERN computer center enough storage media and CPU power to do the reconstruction and analysis of the accumulated data. A preliminary estimate of the CPU needed for the data reconstruction task leads to around 20 000 hours, if done in a current 400 MHz "commodity" PC, like the Pentium II. We could complete the full data reconstruction in a period of three months using the CPU power corresponding to 10 such CPUs.

4 Physics Performance

4.1 Introduction

We have simulated the physics performance of the experiment, using the detector setup described in the previous section. The soft particles were generated according

to thermal distributions, while for hard processes we have used the PYTHIA event generator [15], using the MRS A parametrisation [16] of the parton distribution functions. The muons and hadrons are then tracked through the experimental setup, taking into account multiple scattering and energy loss.

The event reconstruction procedure can be divided in several steps, which are summarised in the following. The first step is the reconstruction of the muon tracks in the dimuon spectrometer, which is performed using a modified version of the standard NA50 reconstruction software package, to take in account the presence of the dipole field in the vertex region.

After the clusterization of the hits in the pixel planes, the reconstruction of all the tracks in the vertex spectrometer is done taking into account the information from the beam-scope (x and y coordinates of the interaction vertex, within ~ 20 μm precision). This allows to reject a large fraction of spurious tracks (random combinations of hits in the pixel planes) and to reduce the computing time needed for pattern recognition by a factor ~ 10.

Using the reconstructed tracks, the interaction vertex is fitted using the weighted gaussians sum method, which suppresses the "outlier" tracks (tracks which do not converge to the interaction point). Already at this stage most of the muon tracks oroginated from π and K decays are suppressed. In fact, many of the muons coming from hadrons which decay within the vertex spectrometer correspond to tracks not pointing to the vertex and are therefore rejected during this reconstruction step.

Among all the tracks reconstructed in the vertex telescope, the candidates to match the muons measured in the dimuon spectrometer are selected. The selection criterium is based on the comparison of the angles and momenta of the tracks as measured in the two spectrometers. A "matching χ^2" is defined as the weighted square of the differences of the curvature (inversely proportional to the momentum) and of the slopes in the $x - z$ and $y - z$ planes. The tracks with minimum χ^2 are selected.

The matching procedure depends on whether we want to select prompt or displaced vertex (charm decays) muon tracks. In the case of the prompt dimuon analysis, the matching is done on the sample of tracks that point to the vertex. When looking for charm decays, the matching procedure is performed using the tracks which have a minimum offset from the origin.

Among the candidate tracks, together with the real muons we may also have a certain number of hadrons, causing fake matches. This happens when the near by hadrons match the selection criteria as well as the real muon track. Figure 7 shows the matching χ^2 distributions for correct and fake matches.

In the next step the matching candidates are fitted again, this time with the curvature constrained to the value measured in the muon spectrometer, since its momentum resolution is better than the one of the silicon vertex telescope. This step allows to reject some of the fake candidates and improves the precision of the offset measurement, in the y coordinate, to ~ 20 μm.

If the tracks reconstructed in the dimuon spectrometer are decay muons from π or

K mesons that decayed inside the pixel telescope, the vertex spectrometer measures the energy of the parent meson, which is of course always somewhat higher than the energy of the muon. Therefore, a cut on the weighted difference between the energies measured by the two spectrometers, ΔE, provides a further rejection of combinatorial background. Figure 8 shows the simulated ΔE normalized distribution for muons due to ω, π and K decays.

The final mass spectrum contains a certain amount of fake matches, which are then subtracted together with the combinatorial background. The level of fakes contamination can be controlled choosing the cuts to be applied in the matching procedure and depends on the desired relative error on the signal (taking into account the dominating contribution of combinatorial background due to π and K decays).

The mixed events technique is used to subtract both the combinatorial background and the fake dimuons. The combinatorial background spectrum in the measured opposite-sign event sample is determined building a sample of opposite-sign muon pairs composed of muons from different like-sign events. In order to subtract the fake matches, we build a sample of fake dimuons by matching the tracks reconstructed in the muon spectrometer to tracks in the vertex spectrometer which belong to a different interaction. This sample is then normalized and subtracted from the measured mass spectrum. An example of how the fakes subtraction works is shown in Fig. 9, obtained by only generating ω mesons. Besides the event samples before and after subtraction of the fake combinations, the figure also includes the generated distribution, as a reference.

Figure 10 shows the acceptances for $M = 500$ MeV, ω and ϕ dimuons, as a function of the dimuon transverse momentum. The parameters that have the biggest influence on the acceptance are the field intensity of the toroidal magnet, the field in the vertex spectrometer and the hadron absorber configuration. A nice advantage on having a dipole field in the target region is that the low p_{T} muons are bent into the acceptance of the muon spectrometer. This effect can be seen in the p_{T} distributions of accepted ω dimuons shown in Fig. 11, calculated for a current of 3000 A in the toroidal magnet and including 20 cm of iron in the muon filter.

4.2 Low mass dimuon physics

In this section we discuss the results of the simulation related to the study of the low mass dimuons. In this case only the tracks pointing to the interaction vertex are selected. Since most of the π and K decay muons have a significant offset from the interaction vertex, the combinatorial background rejection is more efficient than in the case of the open charm study, discussed in the next section. The reduced sample of matching candidates also results in a smaller contamination from fake matches.

Since we are looking for prompt dimuons, the pairs of matched tracks are fitted with constrained curvatures and the additional requirement of a common vertex point in the proximity of the interaction vertex, in order to achieve the best mass resolution.

Figure 12 shows the mass resolution for the matched dimuons, as a function of

the dimuon mass. For comparison, we also show the mass resolution obtained if we only use the information provided by the muon spectrometer.

The dimuon signal mass spectrum obtained with the proposed detector layout, after subtracting the combinatorial background and fake matches, is plotted on the right side of Fig. 13. The background distribution (including the fakes) is also shown. For comparison, the left side of this figure shows the corresponding spectra if the tracking information of the pixel spectrometer is not used. The normalisation corresponds to one week of data taking, at 10^7 ions/burst, with a target thickness of 10 % $\lambda_{\rm int}$ and a beam efficiency of 75 %. We can clearly see the strong improvement in terms of mass resolution and signal to background ratio.

From these results it is clear that we will be able to distinguish the ω peak from the broader ρ resonance. With the matching cuts tuned in our simulation, 65 % of the dimuon events produced in average centrality Pb-Pb collisions are reconstructed and correctly matched, while suppressing the background by a factor of 12. In these conditions we can collect at least $\sim 200\,000$ ρ, ω and ϕ events per week.

The expected signal to background ratio is around 0.7 in the low mass region (650–850 MeV), considering the combinatorial meson decays and the fake matches. Of course, if the Pb-Pb signal is enhanced by a factor ~ 4, as suggested by the measurements of the CERES collaboration [5], our signal to background ratio would become even better.

4.3 Charm production

For the study of muon pairs from $D\overline{D}$ decays, the pattern recognition and matching procedures are slightly different from the analysis done to study low mass dimuon production. Basically, the final event sample must only contain muon pairs where both muon tracks miss the interaction vertex.

We start by suppressing all the hits belonging to tracks pointing to the vertex and use the remaining points to fit the displaced vertex tracks. In this case, the rejection of combinatorial decay background is less efficient, since the muons from π and K decays also have significant offsets.

In the current analysis, we match only the tracks which have offsets between 110 and 800 μm. This cut rejects a vast majority of the prompt dimuons while retaining $\sim$ 10 % of the $D\overline{D}$ events.

Figure 14 shows the mass spectra for both the open charm selection (left), with both muons in the quoted offset range, and the prompt dimuons (right), where both tracks have offsets less than 80 μm. The background spectrum, including the fake matches, is also shown. These curves correspond to semi-central Pb-Pb collisions (around 200 charged particles per unit rapidity, at midrapidity). The corresponding signal to background ratio, in the mass range $1.2 < M < 2.5$ GeV, is 1:2 in the prompt event sample and 1:6 in the charm sample, for which the reconstruction and matching efficiency is around 10 %.

For dimuon masses above 1.2 GeV and the open charm selection, 90 % of the

signal is due to muon pairs from charmed meson decays, while for the small offset selection, 90 % of the signal comes from prompt dimuons. This procedure will allow us to distinguish which of these two dimuon sources is responsible for the enhanced production of intermediate mass dimuons observed by the NA50 experiment.

5 Results from the Feasibility Tests

In order to check the feasibility of the project, two parasitic tests have been performed in the NA50 experimental area, during 1998. For these tests we used the LHC1 pixel detector, developed by the RD19 collaboration for the WA97 experiment. The LHC1 readout chip is an array of 2048 pixels (128 rows times 16 columns), of dimensions 50×500 μm^2.

We have assembled a test vertex spectrometer, covering the top half muon spectrometer acceptance, with RD19/WA97 pixel chips placed inside the same TC8 dipole magnet we intend to use in the real experiment. The layout is illustrated in Fig. 15, while Fig. 16 shows the experimental area during the November test. The readout electronics can be seen in the front face of the magnet.

It is worth mentioning that some of the chips used to assemble our test telescope were not fully efficient since the beginning. Furthermore, we found that the LHC1 chip was quite sensitive to radiation damage: after few krad the individual channel timings was lost, after $\sim$10 krad it started to suffer from the very inhomogeneous irradiation and after $\sim$30 krad more and more channels got destroyed.

Although these tests were done in very short beam time periods, with a limited geometrical coverage, and with far from perfect reconstruction and matching efficiencies, we could still collect useful data, both with proton and lead beams.

5.1 April 1998

In the April 1998 test run we used the 450 GeV primary proton beam, at 10^8 protons per burst, and a 20 mm beryllium target. In order to increase the acceptance for low mass dimuons, two changes were done relative to the normal running conditions of the NA50 experiment. The 80 cm of iron usually included in the muon filter were removed and the current in the toroidal magnet was decreased from 7000 A to 3000 A.

Out of the dimuon event sample collected in $\sim$60 hours of data taking, 595 opposite-sign dimuon events were correctly reconstructed and matched. Figure 17 shows the corresponding mass spectrum before (left) and after (right) using the pixel spectrometer information to fit the tracks.

The data points are compared to the superposition of two gaussians, representing the ω and ϕ resonances, and a Breit-Wigner, representing the ρ, with relative normalisations imposed from previous measurements (equal cross sections for the ρ and ω mesons and 20 times less ϕ's). Comparing the two figures, we clearly see a substantial improvement in mass resolution: the curves on the left have $\sigma(\omega) = 70$ MeV and

$\sigma(\phi) = 75$ MeV while those on the right have $\sigma(\omega) = 23$ MeV and $\sigma(\phi) = 26$ MeV. These values are in good agreement with the expectations from the simulation.

5.2 November 1998

In November 1998 we had a 3-day test run, sending the Pb beam on a segmented Pb target (three 1.5 mm thick sub-targets spaced by 12 mm). The pixel planes had already suffered from the radiation dose collected during the April test and continued deteriorating during the run, as the radiation load increased.

Figure 18 shows the vertex distribution reconstructed using the tracks measured in the pixel telescope. The number of events and the widths of the three peaks are in good agreement with expectations.

We have simulated the expected performance of the test setup, in terms of single muon track matching, taking into account the measured chip inefficiencies. A comparison between the simulated (left plots) and the measured data (right plots) can be seen in Fig. 19. The top row shows the difference between the slope in the $y - z$ plane for the tracks measured in the vertex telescope and in the muon spectrometer. Similar results were obtained for the $x - z$ plane. The middle row illustrates the quality of the matching in terms of the track curvature.

The bottom row compares the matching χ^2 obtained in the simulated and in the measured data. Not only the shape of the distribution does not reveal any patology in the matching procedure, but also the number of matched muons in the data is in agreement with the simulation results.

The analysis of the collected data is still in progress, but these preliminary results indicate that the detector concept continues to be valid even in the rather demanding conditions of high multiplicity Pb-Pb collisions. In particular, we are now confident that the track matching procedure will work up to the most central Pb-Pb collisions, with efficiencies that can be realistically estimated by simulation.

In the same running period we have also tested a beam-scope prototype with lead ions. We used a silicon pad detector, with 3×3 pads of 1.5×1.5 mm^2 each, operated at 80 K. The lead beam was centered on one pad and we were able to count each incoming lead ion at a maximum intensity of $\sim 5 \times 10^7$ ions per burst. There was no degradation in the detector performance after a few 10^{10} Pb ions passed through the pad, opening good perspectives for the use of this new detector technology for our application.

During 1999 we will perform further tests of this detector, in the NA50 experimental area. In the November 1999 run we will test a final prototype, designed with all the specifications of our beam-scope detector. This work is done with the active support of the CERN RD39 collaboration.

6 Beam requirements and expected event rates

A first estimation of beam time for our low mass dimuon physics programme could comprise two weeks of 450 GeV protons, at around 10^9 protons per burst, for p–Be and p–Pb data, and one week of 158 GeV/nucleon Pb beam, at $\sim 10^7$ ions per burst, with three 1.5 mm Pb targets.

Assuming a trigger rate of 4000 triggers per burst and a beam efficiency of 70 %, we estimate that after one week of Pb running we will have accumulated around 124 000 ω's, 52 000 ρ's and 43 000 ϕ's, with a signal to background ratio of 0.7 in the mass window 650–850 MeV. Such statistics will allow to estimate with good accuracy the ρ/ω ratio and its dependence on centrality (see also the right side of Fig. 13).

For the charm production study we foresee a 30-day Pb run, with a beam intensity of 5×10^7 ions per burst, again preceeded by an adequate proton run. In the dimuon mass window 1.2–2.5 GeV, after applying the offset cut, we expect to keep in the final analysis data sample around 11 000 events. If charm production is enhanced these numbers will be accordingly higher.

The statistical errors are large, due to the dominating combinatorial background from π and K decays in the same offset range. However, the collected data will allow to clarify whether the yield of intermediate mass dileptons scales with the number of nucleon-nucleon collisions (as expected for hard processes) or with the number of participant nucleons, as suggested by the present observations of NA50 [7].

The possibility of also running the experiment with π^+ and π^- beams is currently under study. While charm is mainly produced by gluon fusion, the Drell-Yan cross section is proportional to the squared charge of the annihilating (anti-)quarks. Therefore, the comparison of the dimuon continuum produced with π^+ and π^- beams, on isoscalar targets, should provide complementary information to separate open charm production from $q\bar{q}$ annihilation.

7 Conclusions

In summary, we intend to accurately study dimuon production in proton and heavy ion collisions. Besides measuring dimuon production with a mass resolution of around 20 MeV at the ω mass, we will study the production of charmed mesons by measuring the offset of the muon tracks extrapolated to the interaction point.

The cost of the apparatus is quite modest. Preliminary budget estimates indicate that the new investment money should be around 400 kCHF. The running budget of the experiment should remain around 100 kCHF per year, as in the present NA50 experiment.

The institutes signing this Letter of Intent have all been involved in the running of the NA50 experiment and have the necessary manpower and expertise to maintain the muon spectrometer and the ZDC detector. The preliminary sharing of responsibilities for building and operating the new pixel vertex spectrometer include CERN, LIP and IN2P3. The beam-scope will be made by the CERN group in close collaboration with

RD39. Other groups have expressed interest in joining and we expect little problem in identifying sufficient manpower to construct, operate and analyse the experiment in a timely fashion, following a positive response from the SPSC.

According to the present schedule for the production of the Alice1 chip, we should be able to have the pixel planes ready to be tested in May 2000. A prototype of the beam-scope will be tested in November 1999 and the final detector should be ready in the first half of 2000. Unless we will face unforeseen difficulties, the experiment can be ready for a commissioning run at the end of the ion beam period of year 2000, with the possibility of collecting first physics data. A few weeks of protons in 2001 and one month of Pb ion beam in the year 2002 should be enough to complete our physics programme.

References

[1] P. Braun-Munzinger and B. Müller, Summary report from the meeting "Heavy Ion Physics at the SPS, HIPS-98", Chamonix, France, September 1998.

[2] M.C. Abreu *et al.* (NA50 Coll.), Phys. Lett. **B 410** (1997) 327.
M.C. Abreu *et al.* (NA50 Coll.), Phys. Lett. **B 410** (1997) 337.

[3] M.C. Abreu *et al.* (NA50 Coll.), Phys. Lett. **B 450** (1999) 456.

[4] H. Satz, in "International School of Subnuclear Physics", A. Zichichi (Ed.), Erice, Italy, 1997, BI-TP-97-47, hep-ph/9711289.

[5] G. Agakichiev *et al.* (CERES Coll.), Phys. Rev. Lett. **75** (1995) 1272.
G. Agakichiev *et al.* (CERES Coll.), Phys. Lett. **B422** (1998) 405.
B. Lenkeit *et al.* (CERES Coll.), Proc. INPC-98, Paris, August 1998.

[6] P. Norman *et al.* (WA97 Coll.), XXXIV Rencontres de Moriond, Les Arcs, France, March 1999.

[7] E. Scomparin *et al.* (NA50 Coll.), J. Phys. **G25** (1999) 235.

[8] E.L. Berger, L.E. Gordon and M. Klasen, Phys. Rev. **D58** (1998) 074012.

[9] A. de Falco *et al.* (NA38/50 Coll.), Nucl. Phys. **A638** (1998) 487c.

[10] R. Arnaldi *et al.*, Nucl. Instrum. Meth. **A 411** (1998) 1.

[11] L. Anderson *et al.* (NA10 Coll.), Nucl. Instrum. Meth. **223** (1984) 26.
C. Lourenço, PhD Thesis, Universidade Técnica de Lisboa, 1995.

[12] M. Campbell *et al.*, Proceedings of the "IEEE Nuclear Science Symposium '98", Toronto, Canada, November 1998.

[13] V.G. Palmieri *et al.*, Nucl. Instrum. Meth. **A413** (1998) 475.

[14] L. Casagrande *et al.*, Proceedings of the "IEEE Nuclear Science Symposium '98", Toronto, Canada, November 1998.

[15] T. Sjöstrand, Comp. Phys. Comm. **82** (1994) 74.

[16] A.D. Martin, R.G. Roberts and W.J. Stirling, Phys. Rev. **D51** (1995) 4756.

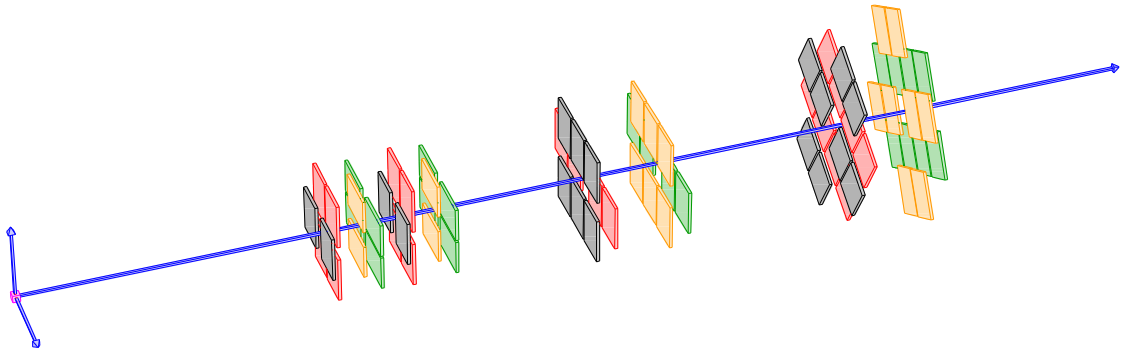

Figure 1: Schematic layout of the silicon pixel vertex telescope.

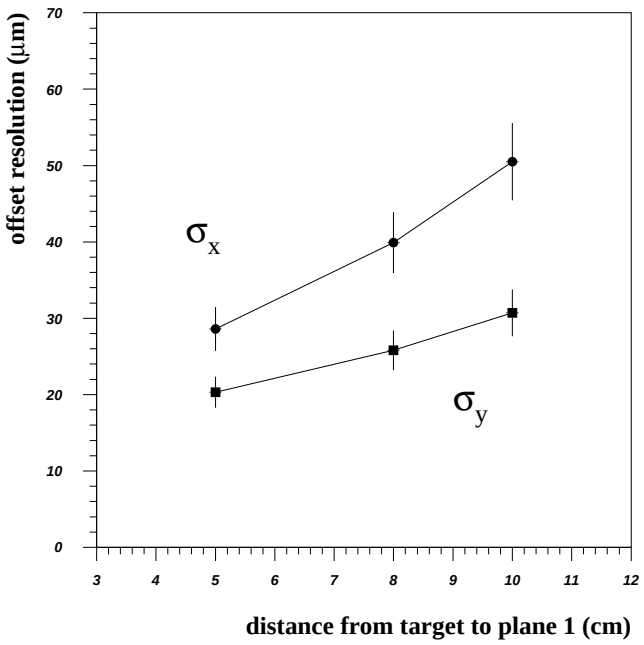

Figure 2: Offset resolution in the x and y coordinates as a function of the z position of the first pixel plane.

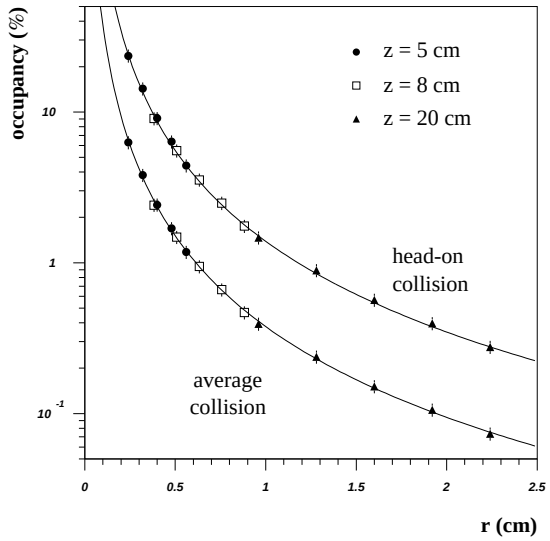

Figure 3: Occupancy as a function of the radial distance from the beam axis, for average and central Pb-Pb collisions.

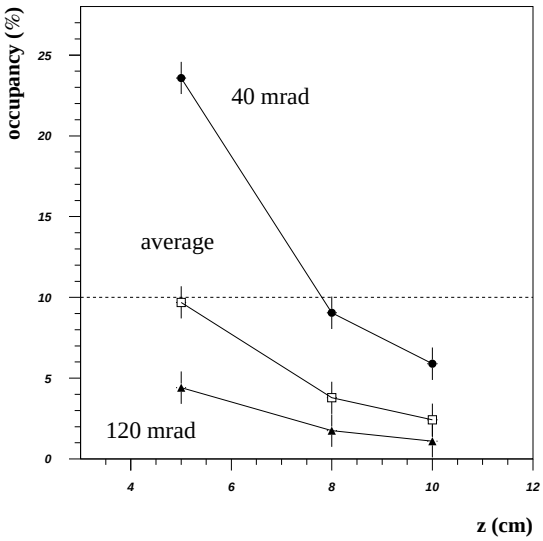

Figure 4: Occupancy for central Pb-Pb collisions, in the angular acceptance of the muon spectrometer.

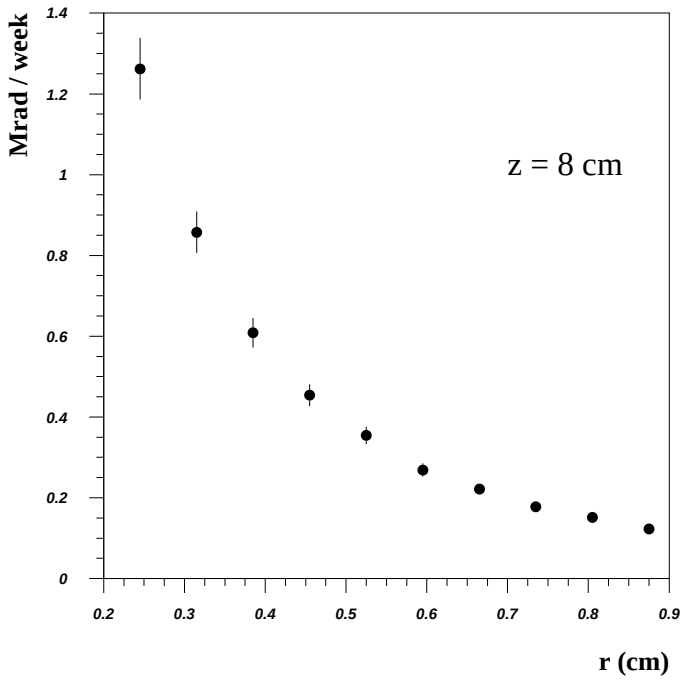

Figure 5: Radiation dose collected by the first plane, placed at 8 cm from the target, as a function of the radial distance from the beam axis. Calculation done for 5×10^6 Pb-Pb interactions per burst.

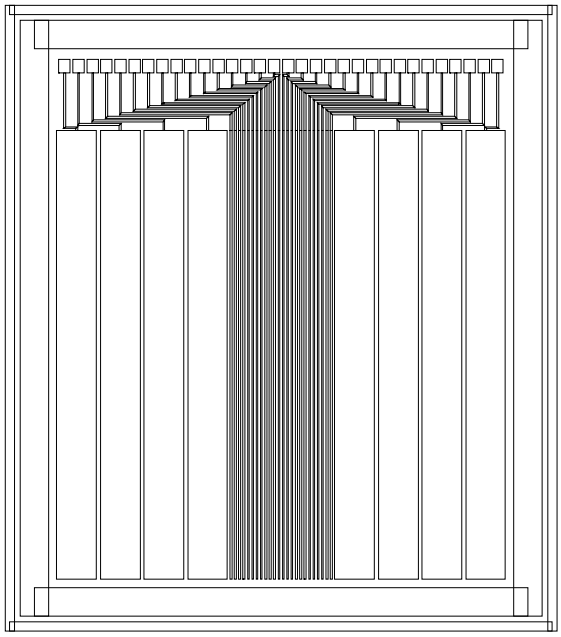

Figure 6: Beam-scope microstrip silicon detector. The pitch is 50 μm in the center and 500 μm on the side, to center the beam.

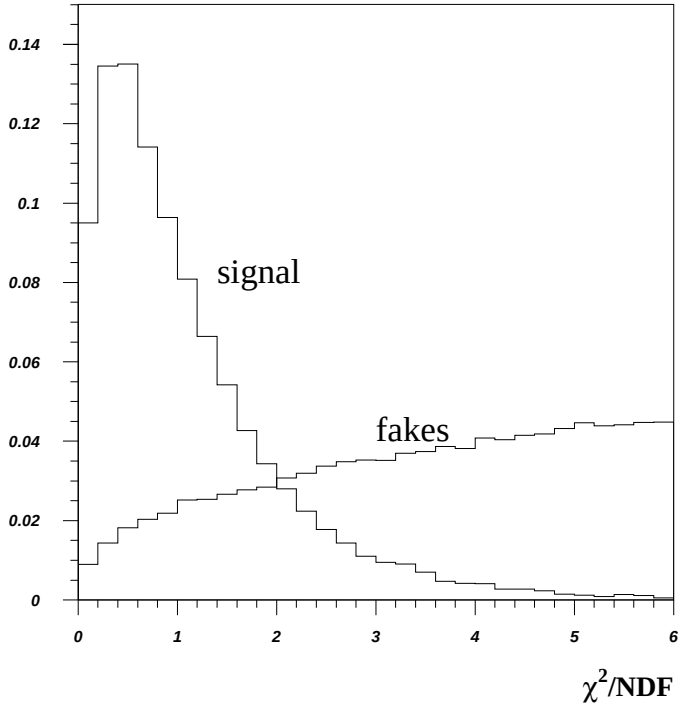

Figure 7: Matching χ^2 normalised distribution for the true and fake matches.

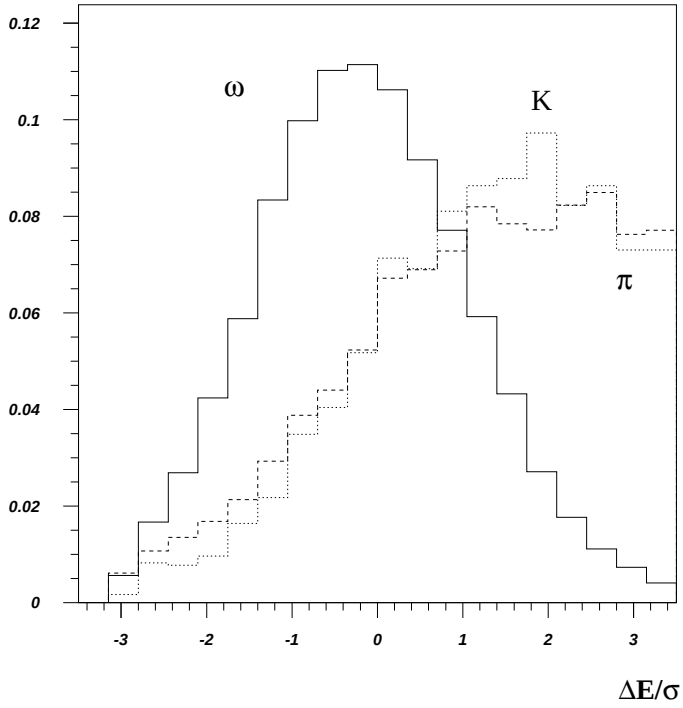

Figure 8: Difference between the energy of the tracks measured in the vertex spectrometer and in the muon spectrometer.

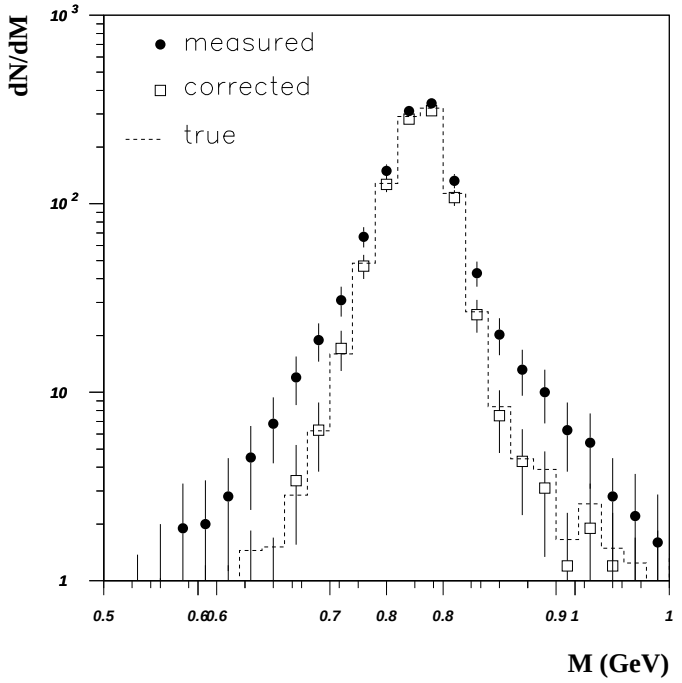

Figure 9: Mass spectrum for generated and matched ω's, before and after subtraction of the fake contamination.

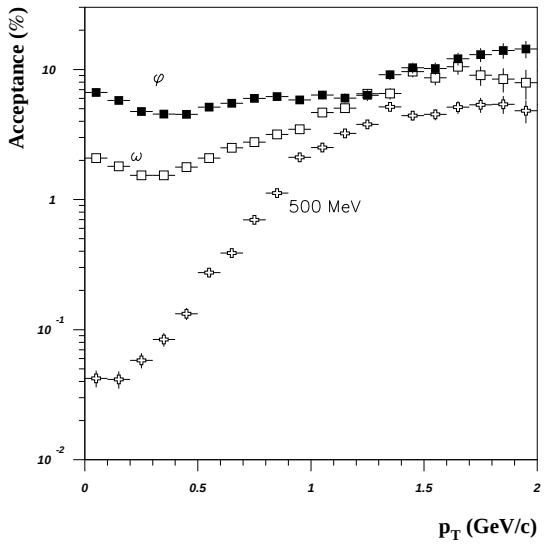

Figure 10: Acceptance versus dimuon $p_{\rm T}$ for ϕ, ω and $M = 500$ MeV dimuons, with the 1.67 T dipole field.

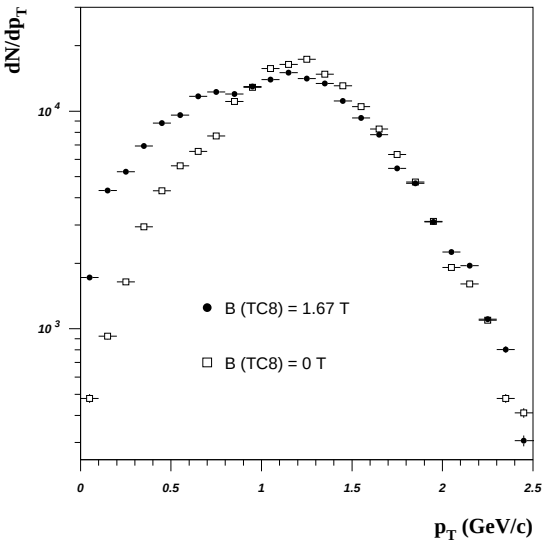

Figure 11: Influence of the vertex magnetic field in the $p_{\rm T}$ distribution of accepted ω's.

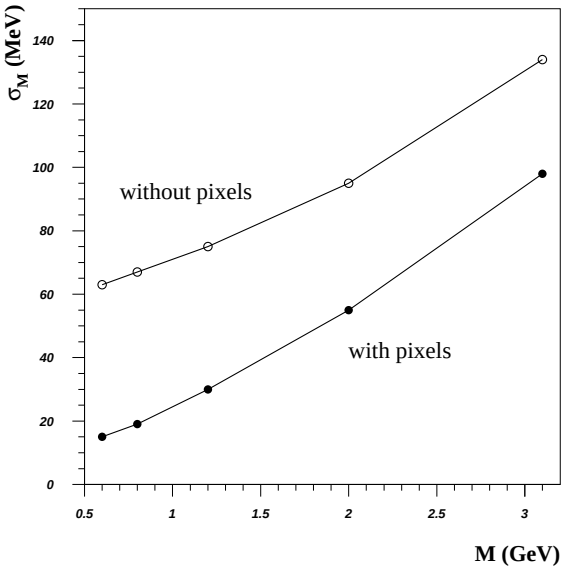

Figure 12: Mass resolution as a function of the dimuon mass, before and after using the pixel telescope information.

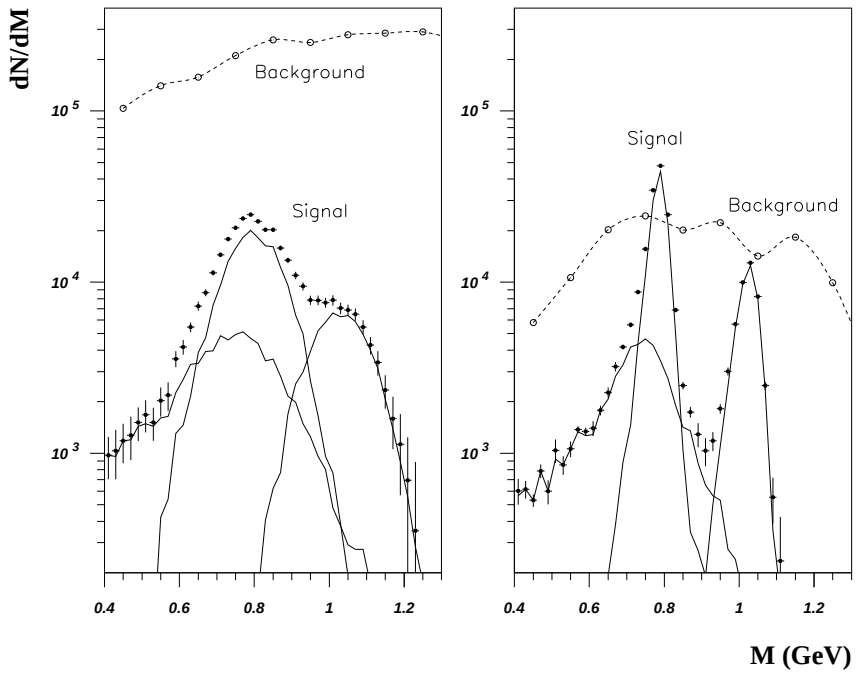

Figure 13: Dimuon mass distribution in Pb-Pb collisions, as measured before (left) and after (right) using the pixel telescope information. On the right plot, the background curve includes the fake matches.

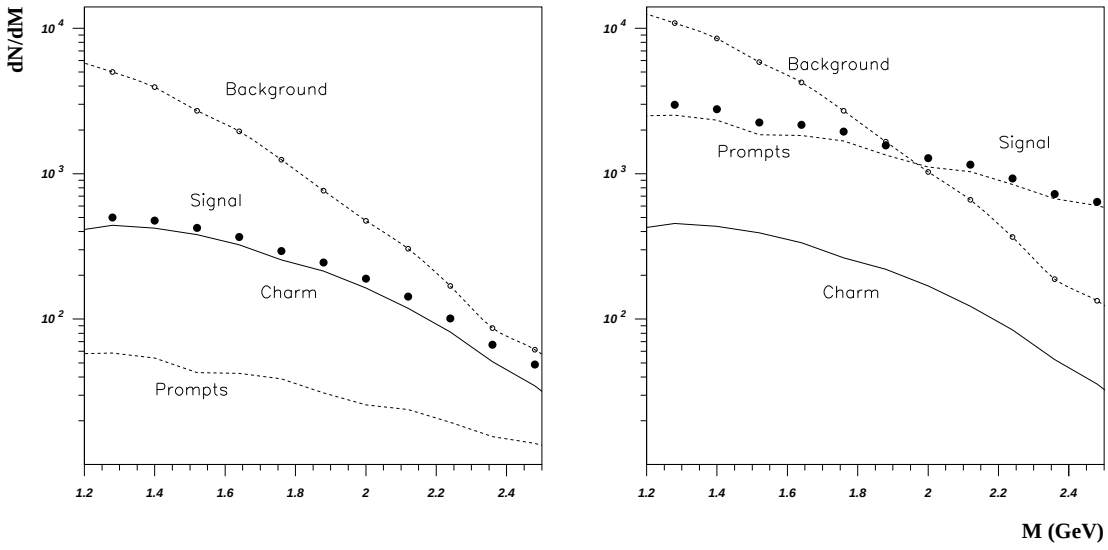

Figure 14: Dimuon mass distributions in two event samples, tagged by the muon track offsets: 110–800 μm (left) and < 80 μm (right).

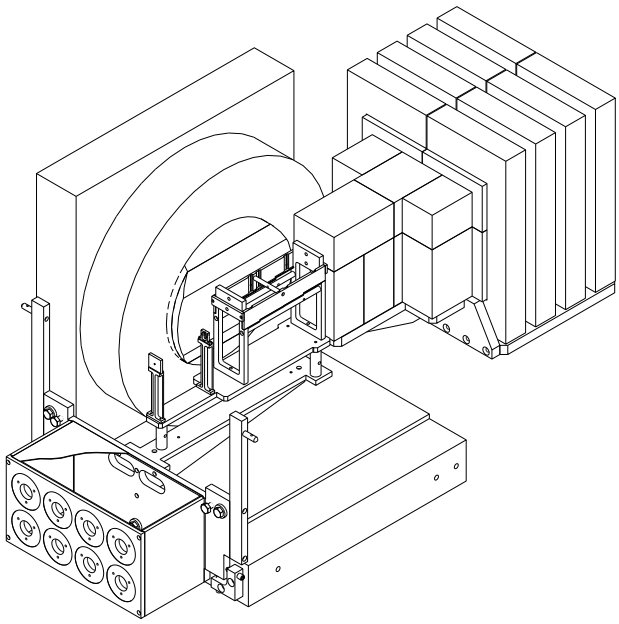

Figure 15: Schematic drawing of the layout used in the 1998 test runs. Along the beam, from left to right: halo counter, target, support box of the pixel planes, and first section of the hadron absorber.

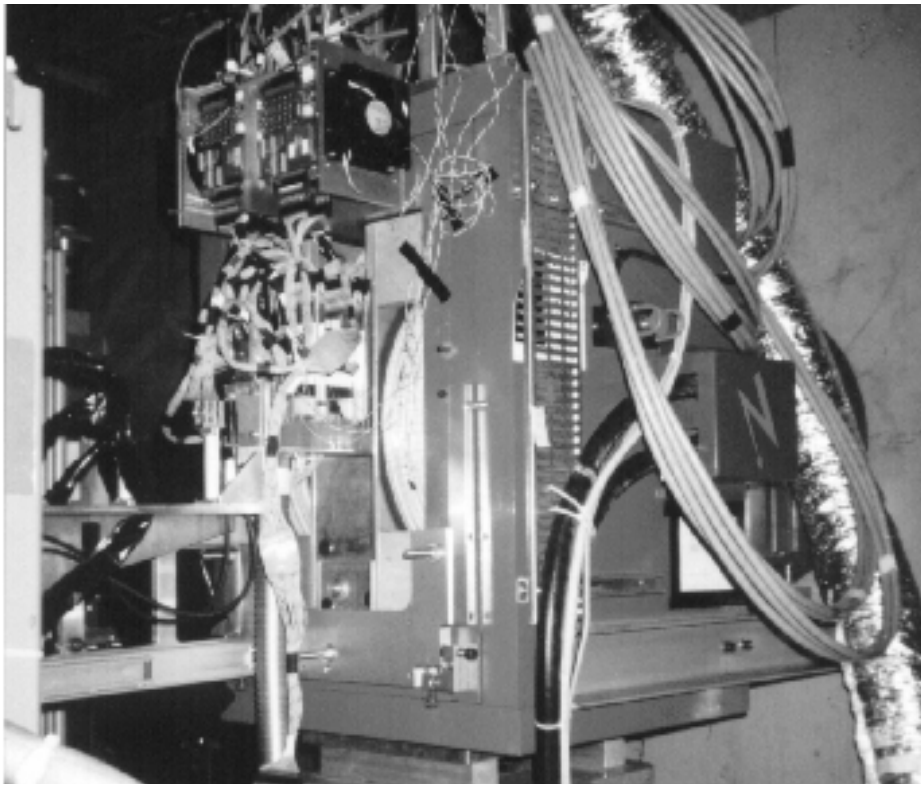

Figure 16: Photo of the experimental area in November 1998.

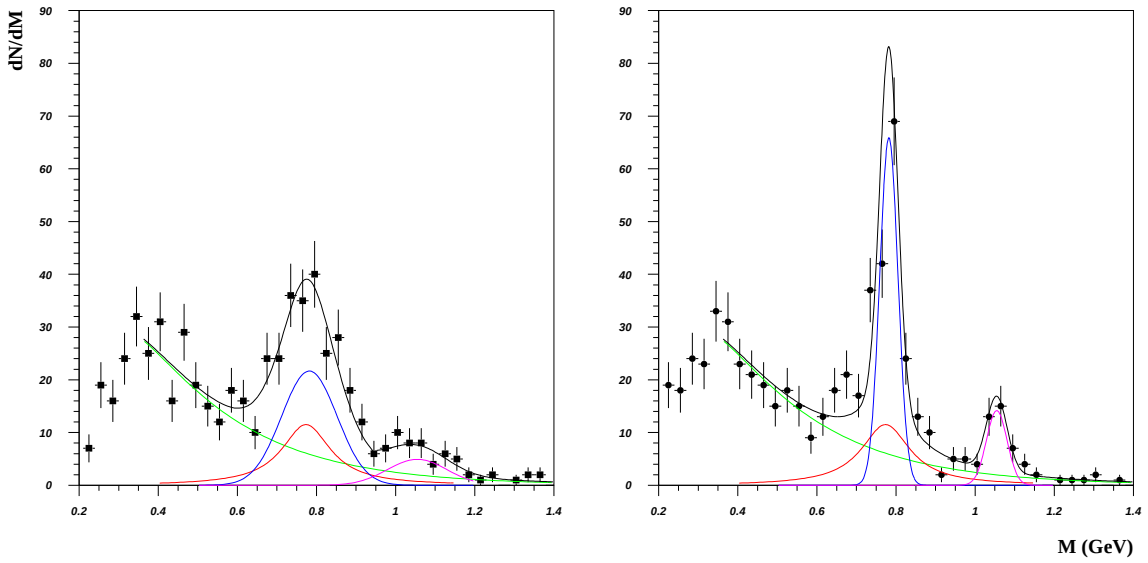

Figure 17: Dimuon mass distribution for p-Be collisions before (left) and after (right) using the pixel telescope information. The curves are normalised to the same number of events in both figures.

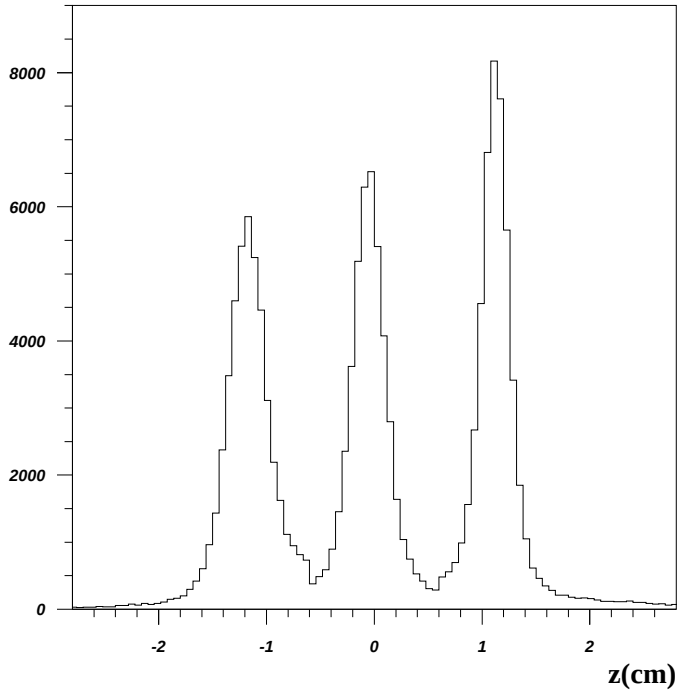

Figure 18: Vertex distribution reconstructed from the Pb-Pb events collected in 1998.

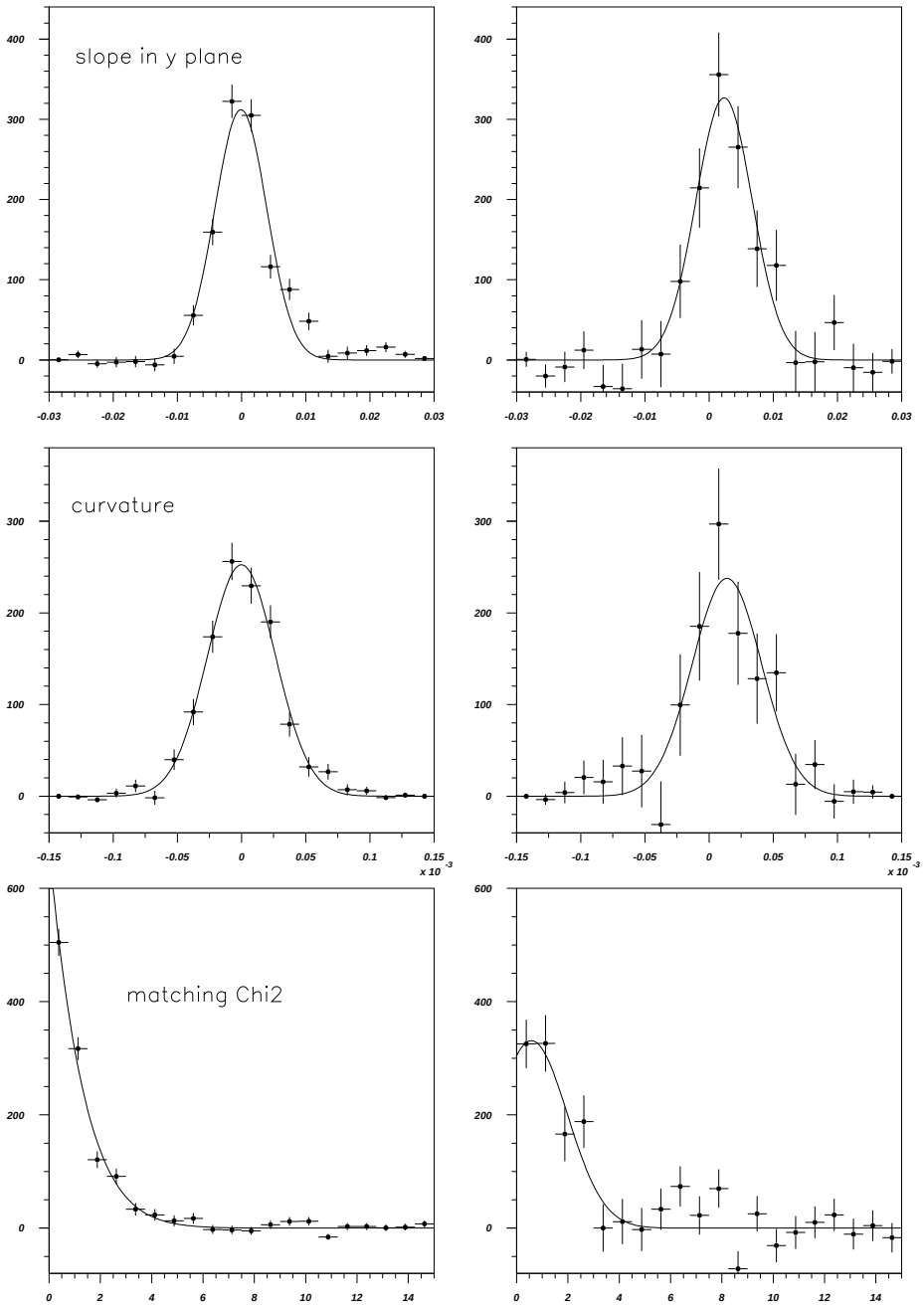

Figure 19: Comparison between the simulated (left) and measured (right) single muon matching parameters.